







RESEARCH ARTICLE

A comparison of established and digital surface model (DSM)-based methods to determine population estimates and densities for king penguin colonies, using fixed-wing drone and satellite imagery

J. Coleman¹ , N. Fenney¹ , P.N. Trathan^{1,2} , A. Fox¹, E. Fox³, A. Bennison¹ , L. Ireland¹, M.A. Collins¹  & P.R. Hollyman^{1,4} 

¹British Antarctic Survey, NERC, High Cross, Madingley Road, Cambridge CB3 0ET, UK

²Ocean and Earth Science, University of Southampton, National Oceanography Centre, Southampton, UK

³Durham University, Durham DH1 3LE, UK

⁴School of Ocean Sciences, Bangor University, Askew Street, Menai Bridge, Anglesey LL59 5AB, UK

Keywords

Counting methods, Digital surface model, DSM, Penguins, Satellite, UAV survey

Correspondence

P. Hollyman, British Antarctic Survey, High Cross, Madingley Road, Cambridge CB3 0ET, UK. Tel: +44 1248 383 594; Email: phyman@bas.ac.uk

Received: 29 January 2024; Revised: 11 October 2024; Accepted: 18 October 2024

doi: 10.1002/rse2.424

Abstract

Drones are being increasingly used to monitor wildlife populations; their large spatial coverage and minimal disturbance make them ideal for use in remote environments where access and time are limited. The methods used to count resulting imagery need consideration as they can be time-consuming and costly. In this study, we used a fixed-wing drone and Beyond Visual Line of Sight flying to create high-resolution imagery and digital surface models (DSMs) of six large king penguin colonies (colony population sizes ranging from 10,671 to 132,577 pairs) in South Georgia. We used a novel DSM-based method to facilitate automated and semi-automated counts of each colony to estimate population size. We assessed these DSM-derived counts against other popular counting and post-processing methodologies, including those from satellite imagery, and compared these to the results from four colonies counted manually to evaluate accuracy and effort. We randomly subsampled four colonies to test the most efficient and accurate methods for density-based counts, including at the colony edge, where population density is lower. Sub-sampling quadrats (each 25 m²) together with DSM-based counts offered the best compromise between accuracy and effort. Where high-resolution drone imagery was available, accuracy was within 3.5% of manual reference counts. DSM methods were more accurate than other established methods including estimation from satellite imagery and are applicable for population studies across other taxa worldwide. Results and methods will be used to inform and develop a long-term king penguin monitoring programme.

Introduction

Drones have been used increasingly to monitor wildlife in recent years (Millner et al., 2023), and therefore the need to process resulting imagery in an efficient manner increases proportionally. Drone survey imagery can be analysed in a variety of ways, from simple manual counts (e.g. Chabot et al., 2015; Mattern et al., 2021) to advanced computer vision approaches such as

convolutional neural networks (e.g. Qian et al., 2023; Torney et al., 2019). Resulting image processing can be a time-consuming and costly process depending on the volume of imagery acquired, the species being monitored, and methods used to count. Modern, fixed-wing drones are a cost-effective tool for large-scale mapping (Budiharto et al., 2019). Their enhanced flight duration allows greater spatial coverage in comparison to traditional multi-rotor drones (Budiharto et al., 2019; Pfeifer

et al., 2019) and their high-resolution sensors allow surveys to be carried out from greater heights, reducing risk of wildlife disturbance. Consequently, fixed-wing drones have great potential for remote applications of wildlife monitoring (Edney et al., 2023; Pfeifer et al., 2019).

The Southern Ocean is experiencing rapid change (Chown & Brooks, 2019; Meredith et al., 2019). Consequently, long-term monitoring data from key sentinel species can provide invaluable tools for assessing ecosystem status and, where appropriate, informing management changes (Bestley et al., 2020). King penguins (*Aptenodytes patagonicus*) are important Southern Ocean predators, that forage in the mesopelagic zone, contributing to biogeochemical cycles both in the ocean (Belyaev et al., 2023) and on land (Burger et al., 1978). Their primary prey are myctophid fish (Olsson & North, 1997), which are likely to see changes in both their distribution and abundance as a result of climate change; such changes are likely to reflect an interplay between physiology (realised thermal niche) and biogeography (latitudinal breeding preference) (Freer et al., 2019). These marine sentinels (Boersma, 2008) are central-place foragers during the breeding season (Watanabe et al., 2023). The productivity and success of the population give information about the status of their surrounding ecosystem (Barbraud et al., 2020). In the Indian Ocean sector, king penguins have been the focus of long-term monitoring for a number of decades (Barbraud et al., 2020; Pascoe et al., 2022), which has revealed significant change, including the rapid decline of the world's largest colony at Ile aux Cochons, Iles Crozet (Weimerskirch et al., 2018) and catastrophic consecutive breeding failures at a large colony on Iles Kerguelen (Brisson-Curadeau et al., 2023). Elsewhere, the recent colonisation of the South Shetland Islands (Petry et al., 2013) indicates a shift in the biogeographic range of king penguins (Cristofari et al., 2018; Le Bohec et al., 2008).

South Georgia is situated south of the Antarctic Polar Front (APF; Fig. 1; Trathan & Murphy, 2003; Trathan et al., 1997). It is a biodiversity hotspot (Atkinson et al., 2001; Murphy et al., 2007) and home to the largest population of king penguins worldwide (Barbraud et al., 2020; Foley et al., 2018). South Georgia waters are protected by a Marine Protected Area (MPA) covering 1.24 million km² (Belchier et al., 2022; Trathan et al., 2014). To date, monitoring of king penguin populations at South Georgia has been opportunistic but it is assumed that they have a latitudinal preference, foraging close to fronts within the Antarctic Circumpolar Current (ACC), primarily the Antarctic Polar Front (APF; Cristofari et al., 2018; Scheffer et al., 2010; Trathan et al., 2008), but also the Southern ACC Front (SACCF; Scheffer et al., 2012). Populations have increased over the last

100 years (Foley et al., 2018; Lewis Smith et al., 1979; Trathan et al., 1996), and with the APF projected to shift, it is likely that population changes will continue to occur (Brisson-Curadeau et al., 2023; Cristofari et al., 2018). Consequently, monitoring population changes is critical (Cristofari et al., 2018; Le Bohec et al., 2008) for a better understanding of changes in the ecosystem status.

Observations of king penguins date back to the early 19th century (Weddell, 1825). Since then, various techniques have been used to quantify colony size, from visual counts (Matthews, 1929) to the use of high-resolution satellite imagery (Foley et al., 2020; Weimerskirch et al., 2018). All methods have both advantages and disadvantages, depending upon the accessibility of the site, the size of the colony and the local terrain. Where colony size is small, visual observations are straightforward, but as colony size increases, levels of uncertainty increase. For larger colonies, oblique photos from vantage points around a colony have been used (Pascoe et al., 2022; Weimerskirch et al., 1992), but these are time-consuming. Satellite imagery is increasingly accessible and affordable, making it possible to track changes in colony footprint over time (Weimerskirch et al., 2018). However, individual penguins are not identifiable in satellite imagery, meaning such methods rely upon estimates of density, and identifying breeding versus non-breeding areas can be challenging (Weimerskirch et al., 2018).

In this study we consider a novel approach to drone image analysis which is neither manual nor computer vision-based, estimating animal counts from post-processed imagery using digital surface models (DSMs). The efficiency and accuracy of this new method are compared to pre-existing manual drone image counting methods, using king penguins as a study species. From this, we then provide recommendations to inform future monitoring protocols. This study also included the first use of fixed-wing drones and the first use of flights Beyond Visual Line of Sight (BVLOS) in South Georgia. We suggest that this method may have wide applicability across many species and habitats.

Materials and Methods

Data collection

King penguins were surveyed in South Georgia using a senseFly eBee X fixed-wing drone. This is a commercially available Remotely Piloted Aircraft System (RPAS) with a maximum flying time of 90 minutes, mounted with an Aeria X, 24 Mega Pixel (MPx), 18.5 mm, RGB sensor. Six king penguin colonies were flown over (Fig. 1): Fortuna Bay (FB), Gold Harbour (GH), Right Whale Bay (RWB), Salisbury Plain (SP), Sea Leopard Fjord (SLF) and St

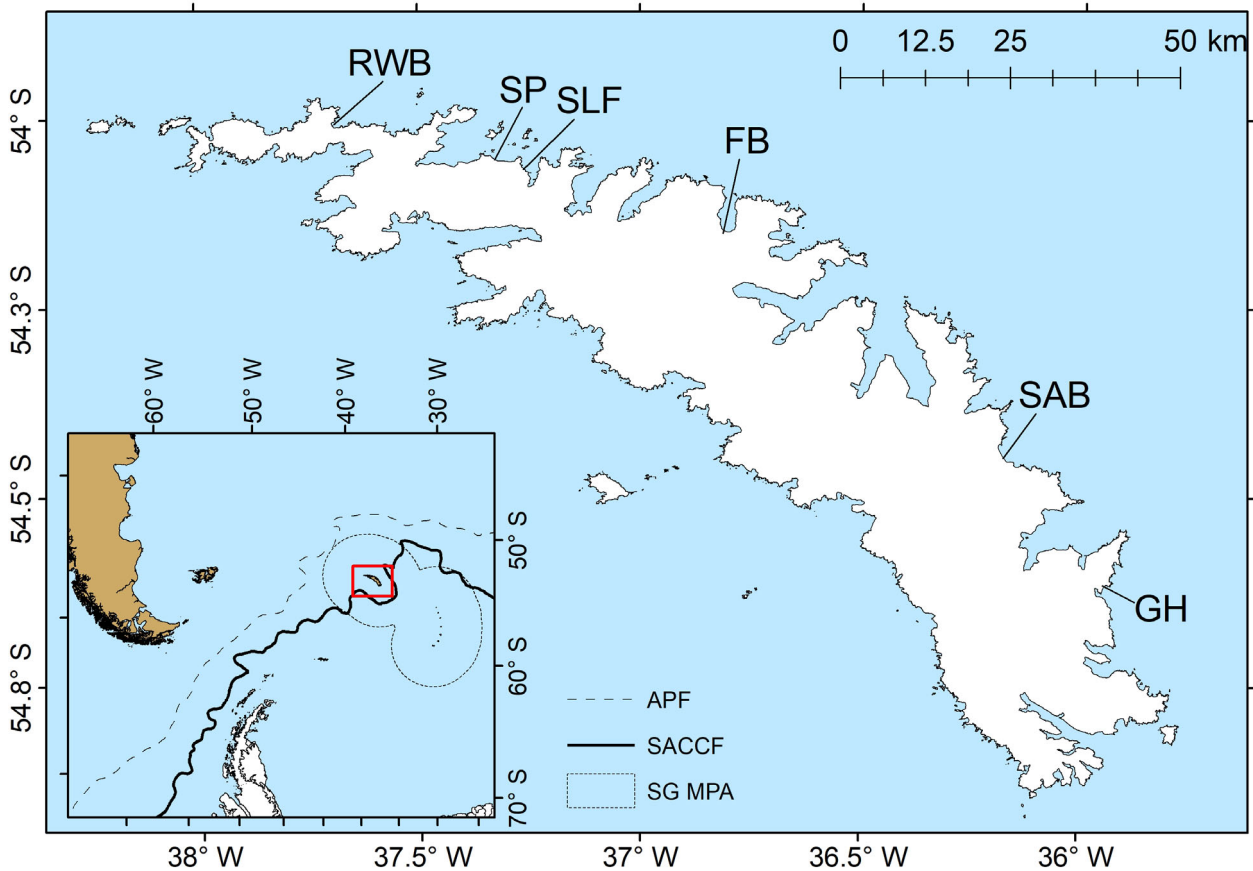


Figure 1. The location of South Georgia and major current systems (inset, APF; Antarctic Polar Front, SACCF; Southern Antarctic Circumpolar Current Front), along with the locations of the sampling sites. (1) Right Whale Bay (RWB), (2) Salisbury Plain (SP), (3) Sea Leopard Fjord (SLF), (4) Fortuna Bay (FB), (5) St Andrews Bay (SAB) and (6) Gold Harbour (GH).

Andrews Bay (SAB). The breeding cycle of king penguins, from laying to fledging, extends over a year (Bost et al., 2013; Stonehouse, 1960) with it commencing for most birds in early spring and finishing late spring the subsequent year. Breeding adults can successfully raise a chick in two out of every three years, though they may attempt breeding in all years (Stonehouse, 1960; Weimerskirch et al., 1992). The duration and timing of the onset of breeding mean that there are two cohorts of breeders within a given colony, leading to challenges in estimating population size (Foley et al., 2020; Pascoe et al., 2022), given variability in the timings of breeding between seasons (Olsson & Brodin, 1997) and between populations (Stonehouse, 1960; Weimerskirch et al., 1992). Counts for estimating peak numbers are best undertaken in January (Bost et al., 2013) but may need to be adjusted (Foley et al., 2020). We undertook surveys in late January (Table 1), to ensure that most breeders were already established, apart from a small number of late breeders (Bost et al., 2013). At this time, only one parent

is usually present. We determined the best time for our surveys using daily ground counts at a small colony (<155 pairs) at Hound Bay in 2005/06 and 2006/07 (Trathan, 2008). After breeding is established, the core colony densities remain approximately constant (Côté, 2000; Gerum et al., 2018) until crèches develop.

Microsoft hybrid satellite imagery and a digital surface model (DSM) derived from NASA Shuttle Radar Topography Mission (SRTM) were used to inform risk assessments and develop flight plans using senseFly eMotion flight planning software. Ground sampling distance (GSD), image overlap (80% forward \times 60% side), flight lines, take-off and landing sites and potential hazards were identified for each colony. To reduce disturbance to wildlife and maximise the survey area, the maximum altitude above ground level (AGL) that provided high (≤ 2 cm) resolution GSD (Table 1) was used. When GSD increased above 2 cm, although the number of pixels per penguin was still high (>140), visual interpretation of imagery became harder (e.g. distinguishing breeding

Table 1. Metadata for drone flights at the six target colonies.

	Fortuna Bay	St Andrews Bay	Gold Harbour	Sea Leopard	Right Whale Bay	Salisbury Plain
Breeding area (m ²)	6,855	85,472	18,905	8,531	12,880	46,592
Date	14-Jan-22	18-Jan-22	21-Jan-22	22-Jan-22	22-Jan-22	23-Jan-22
Survey Length (km)	14.5	25.7	12.7	5.3	7.0	16.5
Survey Time (mins)	19	35	17	8	10	23
Flight Altitude (m)	94.6	89.9	85.2	85.2	85.2	85.2
Targeted GSD Resolution (cm)	2.0	1.9	1.8	1.8	1.8	1.8
Orthomosaic Resolution (cm)	2.1	1.9	1.9	1.9	1.8	1.8
DSM Resolution (cm)	4.0	3.7	3.7	3.9	3.7	3.6

versus loafing penguins). Greater altitude allowed for rapid mission times within weather gaps and in fading light, which was often when wind speed was lower. Primary take-off and landing sites were chosen as areas that were flat, away from colonies (300 m to 3000 m distant), provided a good vantage point of the site and were remote from any hazards such as boulders and other wildlife. On site, further risk assessments were undertaken based on the topography, wind speed and wind direction, which then dictated the orientation of flight lines. All flights were undertaken with a drone operator and two observers.

Prior to all flights, a Trimble R9s global navigation satellite system (GNSS) base station was established. The Canadian Spatial Reference System Precise Point Positioning (CSRS- PPP) service gave International Terrestrial Reference Frame (ITRF) solutions for the base station. This position and the base station GNSS data were then used as the origin for post-processed kinematic (PPK) processing of the onboard GNSS data for the drone track, giving better accuracy (<5 cm) positions for the camera. This then allowed a DSM to be generated by Agisoft LLC's Metashape (version 1.8.4 build 14671) photogrammetry software. The DSM was generated from a dense point cloud (medium-quality setting) following initial image alignment (high-quality setting). Finally, the images were mosaicked and orthorectified using the DSM and each dataset was referenced to a Universal Transverse Mercator (UTM) 24S projection.

Counting methods (see Fig. S1 for workflow)

Full manual count (SL only)

The orthomosaic for Sea Leopard Fjord was opened in ESRI ArcGIS Pro (version 3.0.0) where every bird considered to be breeding was identified by a single observer and recorded in a point shapefile as an observation.

Breeding birds were standing at regular distances from each other (beyond peccable distance e.g. ~0.6 m). Where two adults were present, side by side within breeding areas, they were assumed to be a breeding pair and only one was counted. Birds standing next to juveniles (pre-fledging chicks) were ignored and considered to be breeders from the previous year. To reduce processing time, the DSM method was used to assist subsequent manual counts (see DSM-assisted manual counts below).

DSM-Based Counts

Semi-automated digital surface model counts (See Fig. S2 for workflow)

For each of the six sites, DSMs were produced in a raster file format (Table 1). A high-pass *filter* (ArcGIS Pro function) was applied to each DSM, and a binary raster was generated from the filtered DSM using the 'raster calculator' function to conditionally classify each point above or below a certain value (e.g. Con('filteredDSM' > 0.1,1)). The resulting raster highlights clusters of points of higher elevation (penguins) on the DSM. The classification threshold to highlight these points varied between sites. Different thresholds were trialled with a number selected (between 0.045 and 0.15) which balanced minimising noise against selecting as many penguins as possible. Rasters were then converted to point shapefiles using the 'raster to point' function, with multiple points representing penguins from which point clusters could be grouped using the self-adjusting clustering method in the 'density based clustering' function. These were then extracted as single points using the 'feature class to point' function from the centre of the 'minimum bounding geometry'. All penguins outside the known breeding areas and within gaps were then removed. Where paired penguins were standing next to each other, two points were present. These paired points were reduced, to one, using a distance filter of 40-45 cm in the CloudCompare software (Version 2.12.3 – Kyiv).

These distances were calculated based on the density of each colony.

Although not necessary at sites where DSM resolution produced accurate counts, automated counts (using the DSM approach described above) based on 15×15 m quadrats were compared to manual counts to give a correction factor for missing birds. Five quadrats were used at FB, SLF and RWB; ten at GH and SP and 15 at SAB. At SAB, there were three small gaps in the DSM, as a result of gusting wind during part of the flight causing a loss of stereo cover in the images, but birds in these areas were counted manually from the drone imagery and added to the DSM automated count.

Manually adjusted DSM count

At the four sites (SLF, RWB, GH and FB), with the best quality imagery, subsequent to the semi-automated DSM counts (see above), a small number of missed birds were manually counted, until a full colony count was achieved.

Density-Based Counts

Quadrat-based counts

ArcGIS Pro was used to annotate orthomosaics. For each site, polygon shapefiles were manually drawn around areas of breeding birds to calculate breeding area (m^2). For non-breeding spaces, within colony areas, further 'gap' polygons were generated with this space subtracted from the initial breeding area. For each colony, a number (between 5 and 15, colony size dependent) of 15×15 m squares ($225 m^2$) were randomly placed within the site using the 'Create Random Points' tool in ArcGIS. Each breeding pair within the quadrats was tagged by two observers using a point shapefile to give a quadrat count. These allowed individual and average quadrat densities to be computed for each site. Average quadrat densities were then applied to the total breeding area to give a colony estimate.

Quadrat modelling with core

For colonies where we generated manually adjusted DSM counts, each penguin was associated with a georeferenced point within a manually drawn colony area polygon. These were used to test the accuracy and efficacy of quadrat counting methods. Multiple 25, 100 and $225 m^2$ square quadrats were overlaid on colony outlines and every penguin counted within the quadrats. Only quadrats whose entire area fell within the colony were used. Using R studio (Version 1.3.1056), n number of

quadrats were randomly subsampled to estimate the colony population. Population estimates and 95% confidence intervals were calculated from mean density in n quadrats and multiplied by the colony area. This procedure was repeated from 1 to 200 quadrats to test how many of each size were needed to reduce errors associated with density-based estimates. The median and 95% confidence intervals were then plotted for the first 200 replicates.

Quadrat modelling with buffer and core

To account for differences in density between the colony edge and core, a 3 m buffer area was created on the colony perimeter. Grids of 25, 100 and $225 m^2$ quadrats were overlaid on the colony perimeter as above. This grid was then divided at the 3 m buffer, giving a buffer grid and a core grid. For the core grid, only whole quadrats were used. However, this was not possible for the buffer grid due to its 3 m width. Here, for the $25 m^2$ grid, all quadrats less than $10 m^2$ were removed, for the $100 m^2$ grid all quadrats less than $25 m^2$ were removed and for the $225 m^2$ grid, those smaller than $50 m^2$. All penguins within quadrats were counted. The same function used in quadrat modelling was then used to generate plots for both buffer and core subsamples.

Density variability and colony slope

Using manually adjusted DSM colony counts from SLF, FB and RWB, two methods were applied to assess change in density across the colonies to better understand the limitations of density-based estimates. First, a kernel density plot was produced, using the Kernel Density tool in ArcGIS, to show the changing densities of penguins across $3 m^2$ areas. Then polygons were produced around each penguin in ArcGIS Pro (using the Create Thiessen Polygons tool to draw Voronoi cells), which gave the area of space closest to each penguin. Each penguin not bordering the colony edge was assigned an area of personal space (the area closest to the penguin) and a distance from the colony edge to see how density changed across the site.

At RWB, where part of the colony lies on a terrain gradient, the average slope of the surrounding 1 and $5 m^2$ was calculated, for each penguin, from the DSM. To do this, a filter (ArcGIS spatial analyst 'Filter' tool) was used to remove penguins from the DSM before utilising the slope function in ArcGIS. The low pass option was used which applies a 3×3 pixel filter to the raster. Both area and gradient were log-transformed and a linear regression model was used to test the significance of the relationship between them.

Satellite counts

Satellite images were only available for SL and SP. At these sites, panchromatic and multichromatic high-resolution Maxar WorldView III satellite images were captured on the 22nd January (SL) and 31st January 2022 (SP) and imported into ArcGIS. They were orthorectified using both the reference elevation model of Antarctica (REMA, Howat et al., 2022) and the drone-generated DSM. Both resulting images were then pansharpened. The breeding colony was identified using existing waypoints (Trathan et al., 1996) and confirmed by the presence of birds in imagery. Breeding area polygons were manually drawn from the resulting output image. The population was estimated using breeding densities calculated from the 15 × 15 m quadrats (see density-based counts for details). Estimates were compared to the most accurate value available for both sites, quadrat-based counts.

Results

Drone surveys

Flight durations lasted between 8 minutes (SLF) and 35 minutes (SAB); Table 1. All flights were flown at altitudes between 85 m and 95 m achieving a GSD of 1.8–2.0 cm per pixel. Beyond Visual Line of Sight flying was used at all sites with the FB colony flown from the furthest, ~3 km distance. This was because of access limitations, restricting pilots from the colony.

Due to time and weather constraints, it was not always possible to fly in optimal conditions. Low cloud at SP reduced the resolution of the DSM and produced lower image quality whilst gusting wind at SAB led to small gaps in the DSM. However, sufficient imagery meant orthomosaics could still be completed. These were produced for each of the sites allowing polygons to be generated for colony outlines and quadrats to be drawn for subsampling and estimating densities (Fig. 2a). Sites varied in composition with SAB comprising 48 separate sub-colonies compared with FB which only had two. At SLF, there were no 'gap' areas of non-breeding birds. At SP gaps made up 5,861 m² (12.6%) of the breeding space.

Full manual count

The only full manual count was for the SLF colony. Breeding penguins within the SLF colony were annotated giving 13,489 breeding pairs. This process took a single observer 24 hours of effort. At GH, SLF, RWB and FB the DSM method was used to assist manual counts (see

manually adjusted DSM count below) and was considered the most accurate estimate for colony size to compare other estimates against.

Digital Surface Model Counts

Semi-automated DSM-assisted count

At all sites, penguins were easily distinguishable in the DSMs (Fig. 2b). Small gaps in the DSM were present at SAB and resolution was lower at SP. However, automated counting detected penguins at each of the sites. Initial passes resulted in estimates within 5% of the colony count except for SP where reduced visibility impacted image quality in places, resulting in undercounting (−14.4%).

DSM quality was sufficient at GH and SLF so that 99% of birds were automatically counted. At other sites, after DSM counts were adjusted using the quadrat counts, colony estimates for RWB and FB fell within 1% of a manually adjusted DSM count (Table 3). The adjusted SP and SAB estimates were both lower than quadrat-based estimates (SAB 0.2% and SP 3.5%). At all sites, DSM estimates were lower than density-based estimates.

Manually adjusted DSM count

Full DSM-assisted manual counts were made at four of the colonies (GH, SLF, RWB and FB). These were treated as reference counts from which densities were calculated and other estimates were compared (Tables 2 and 3). At GH, 28,751 pairs were estimated, compared with 10,466 pairs at FB, 13,600 pairs at SLF (111 more than full manual count) and 20,012 pairs at RWB. At each of these four sites, DSM-assisted counts were lower (2.5%–4.8%) than numbers estimated by 225 m² quadrats.

The greatest density was observed at SLF where there were 1.594 birds per m² compared to 1.521 at GH which had the lowest density of these four colonies. All actual densities were below those calculated from quadrats. However, when ranked they followed the same order. Given the relationship between quadrat densities and actual density, SAB likely had the lowest density.

Density-Based Counts

Quadrat-based counts

Quadrat density varied between sites, with the mean number of penguins per 225 m² quadrat ranging from 346 at SAB (1.54 penguins per m²) to 367 at SLF (1.63 penguins per m²). Density between quadrats also varied across individual colonies, the greatest variation was at

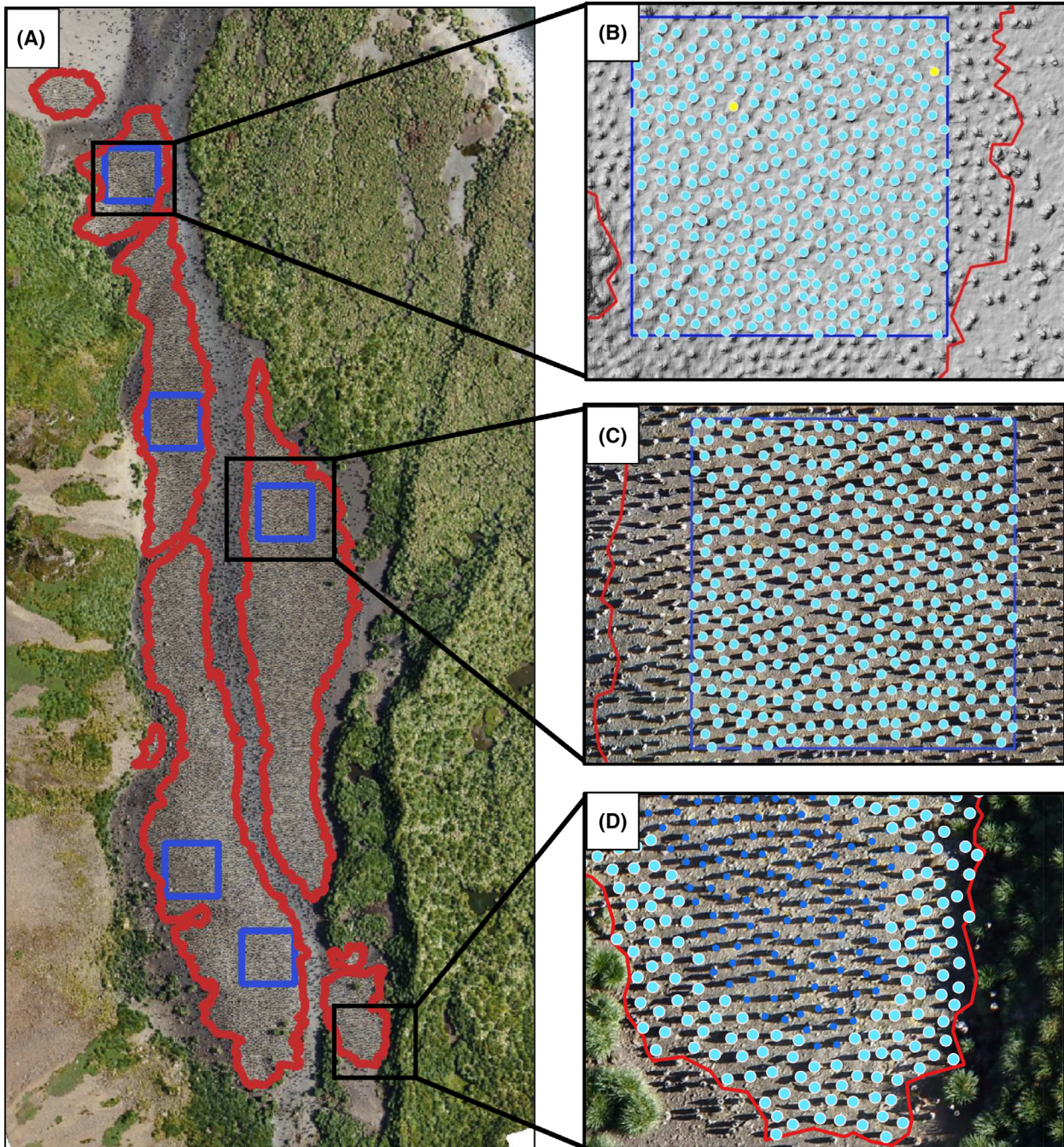


Figure 2. (a) Orthomosaic of Sea Leopard Fjord with colony outlines (red) and 225 m² quadrats (blue) marked. (b) DSM imagery with automated counted penguins in light blue and missed penguins highlighted in yellow. (c) Quadrat with each penguin pair marked manually in light blue. (d) 3 m colony buffer with penguins counted highlighted in light blue; the penguins in the central part represent the higher density 'core'.

RWB ($SE = 0.042$) and the least at FB ($SE = 0.011$). There was a weak negative correlation between colony size and penguin density; however, this was not significant (Pearson's correlation, $r^2 = -0.65$, $df = 4$, $P = 0.165$).

Quadrat-based colony estimates ranged in size from 11,919 breeding pairs (FB) to 132,577 breeding pairs (SAB). At colonies with reference population counts (i.e. manually adjusted DSM colony counts); estimations using

Table 2. Colony estimates with 95% confidence intervals calculated from subsampling of 5 × 5 (25 m²), 10 × 10 (100 m²) and 15 × 15 (225 m²) quadrats across Fortuna Bay, Sea Leopard Fjord, Right Whale Bay and Gold Harbour.

	Number of subsamples	Mean breeding pairs	Upper Confidence Interval	Lower Confidence Interval	Actual Count	Percentage from actual
Fortuna Core 25 m ²	30	10575	12263	8886	10466	1.04
Fortuna Buffer 25 m ²	30					
Fortuna Core 100 m ²	8	10601	11700	9503		1.29
Fortuna Buffer 100 m ²	8					
Fortuna Core 225 m ²	4	11327	12764	9890		8.23
Fortuna Buffer 225 m ²	4					
Fortuna 25 m ²	30	10672	12974	8369		1.97
Fortuna 100 m ²	8	10942	11649	10236		
Fortuna 225 m ²	4	10895	11219	10571		4.10
SL Core 25 m ²	30	13578	15438	11719		13600
SL Buffer 25 m ²	30					
SL Core 100 m ²	8	13353	14778	11928		
SL Buffer 100 m ²	8					
SL Core 225 m ²	4	13519	14713	12325		
SL Buffer 225 m ²	4					
SL 25 m ²	30	13735	15718	11753		
SL 100 m ²	8	13943	15033	12854		2.53
SL 225 m ²	4	13849	14456	13241		
RWB Core 25 m ²	30	20106	24451	15761	20012	0.47
RWB Buffer 25 m ²	30					
RWB Core 100 m ²	8	20293	23629	16957		1.40
RWB Buffer 100 m ²	8					
RWB Core 225 m ²	4	20993	22259	19727		4.90
RWB Buffer 225 m ²	4					
RWB 25 m ²	30	19801	23488	16114		-1.06
RWB 100 m ²	8	21333	25800	16865		
RWB 225 m ²	4	21606	23932	19280		7.97
Gold Core 25 m ²	30	28724	33741	23707		28751
Gold Buffer 25 m ²	30					
Gold Core 100 m ²	8	28906	32807	25005		
Gold Buffer 100 m ²	8					
Gold Core 225 m ²	4	30021	32342	27700		
Gold Buffer 225 m ²	4					
Gold 25 m ²	30	29013	32974	25051		
Gold 100 m ²	8	29408	32960	25855		2.28
Gold 225 m ²	4	29744	34628	24860		

Note: Estimates from entire colony sampling as well as separate core and buffer sampling are presented.

average densities from the 225 m² quadrats all overestimated colony size but lay within 5% of the reference count (2.5% at SLF to 4.8% at RWB). At SP and SAB, where manually adjusted DSM counts were not available, this method was treated as the reference count.

Quadrat modelling of entire colony

At all sites, when using 25 m² quadrats, the variation in mean density, and therefore colony population estimate, reduced after 30 quadrats to the point where additional

samples did not significantly alter population estimates (Fig. 5). This equated to subsampling 750 m² of the colony and didn't change with colony size. Similarly, using 15 replicates of the 100 m² quadrats, equating to 1,500 m², led to similarly stable estimates. Using 15 replicates of the 225 m² quadrats, equating to 3,375 m², led to more stable population estimates. These sampling analyses equated to a high proportion of smaller sites (FB = 7,058 m²). As such, comparing colony estimates using the equivalent cumulative area of 30 × 25 m² (750 m²) (Fig. 5 and Table 2) is most efficient.

Table 3. Summary of count estimates for six king penguin colonies with percentage difference from the most accurate estimate (highlighted in red) marked in brackets.

	Fortuna	Sea Leopard Fjord	Right Whale Bay	Gold Harbour	Salisbury Plain	St Andrews Bay
Manually Adjusted DSM	10,466	13,600	20,012	28,751		
Full manual		13,489 (−0.8%)				
Core + Buffer (25 m ² quadrat)	10,575 (+1.0%)	13,578 (−0.2%)	20,106 (+0.5%)	28,678 (−0.3%)		
25 m ² quadrat entire	10,671 (+2.0%)	13,735 (+1.0%)	19,800 (−1.1%)	29,012 (+0.9%)		
DSM Count	10,181 (−2.7%)	13,511 (−0.6%)	19,357 (−3.3%)	28,458 (−1.0%)	64,837 (−13.7%)	131,419 (−0.9%)
DSM-Corrected Count	10,492 (+0.2%)	13,674 (+0.5%)	20,554 (+2.7%)	29,031 (+1.0%)	72,674 (−3.5%)	132,251 (−0.2%)
225 m ² Density	11,919 (+4.3%)	13,945 (+2.5%)	20,962 (+4.8%)	29,786 (+3.6%)	75,272	132,577
Untrained Satellite Count		17,046 (+22.2%)			102,583 (+36.3%)	
DEMA Satellite Count		16,213 (+19.2%)			103,395 (+38.1%)	
Satellite Count		15,736 (+12.8%)			93,098 (+23.9%)	

Note: Where a full colony, manually adjusted DSM count was not available, density-based counts are considered to be the most accurate.

At all four sites, colony size was estimated to be within 2% (FB +1.97% above actual colony size, SLF +0.99%, RWB −1.06% and GH, +0.91%) of the reference count using 5 × 5 (25 m²) quadrats. At all four sites, as quadrat size increased, colony estimates became increasingly inaccurate, with a trend of overestimating, although confidence intervals decreased. Confidence intervals were greatest using the 5 × 5 (25 m²) quadrats.

Quadrat modelling of buffer and core

Variance across all four sites using buffer and core grids was reduced when subsampling the smallest area of 5 × 5 (25 m²) quadrats (30 subsamples, Fig. S3). At all sites for each of the quadrat sizes, using a combination of core and buffer areas, estimates were more accurate than quadrat sampling the entire colony area and the 25 m² core and buffer estimates were the most accurate (Table 2).

Density variability

Voronoi densities were produced (Fig. 3b) for SLF ($n = 12,043$), RWB ($n = 17,322$) and FB ($n = 9,484$). The amount of 'personal' space assigned to each penguin varied between sites and throughout colonies. On average, birds closer to the colony edge were assigned greater areas than those closer to the core. This relationship was not uniform across the colony (Fig. 3a). However, penguins on the periphery (3 m buffer) of the colony had markedly

lower density than those in the colony centre, 'buffer effect' (Fig. 3c).

The percentage of total colonies that the buffer represented varied from 24.5% at SP to 42.8% at SLF. Quadrats at SLF occupied the greatest percentage of the buffer area (11.8%) followed by GH (6.5%), FB (2.4%) and RWB (2.4%). Densities within SLF quadrats were closest to the actual density calculated from the manually adjusted DSM counts (Table S1; quadrat = 1.63, actual = 1.59).

Slope

Although slope analysis showed high variability, a linear regression showed that there was a significant relationship between penguin density and slope ($P < 0.001$). As the slope increased, the personal space around nesting penguins (Voronoi size) also increased. Despite having a gradient across much of the site, overall density at RWB fell within the range seen at the other six sites.

Satellite counts

Satellite imagery from SLF and SP were available respectively for the same day as drone flights or the day before. GSD of the satellite imagery was 0.6 m at SLF and 0.37 m at SP (Fig. 4), with reduced GSD at SLF due to low, thin, cloud cover. Even with greater resolution at SP, it remained difficult to identify spaces occupied by

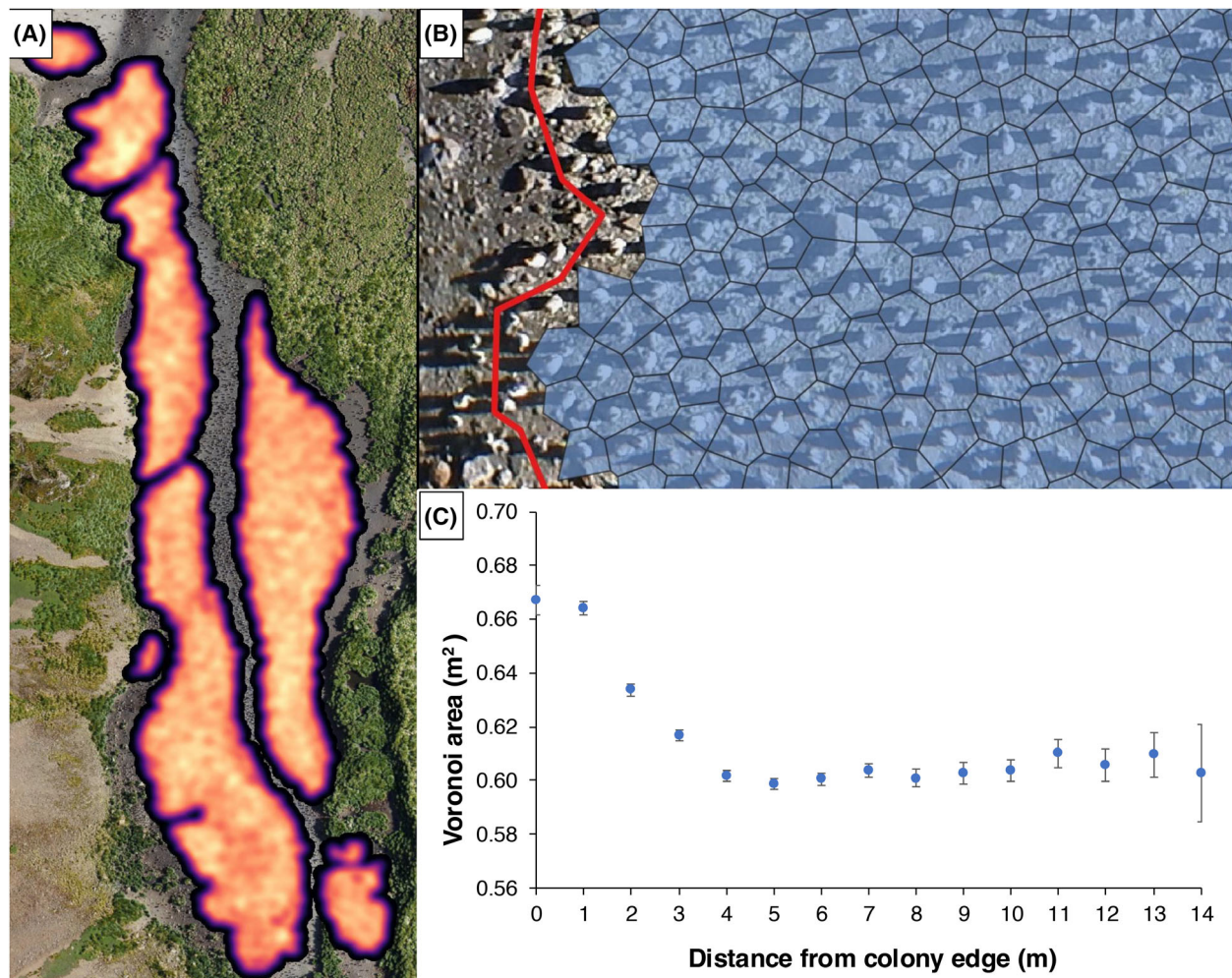


Figure 3. Density variations across Sea Leopard Fjord: (a) Kernel density plot of penguin density where yellow marks high density, red moderate density and purple, low; (b) Voronoi polygons (blue with black outline) showing personal areas assigned to penguins; (c) Plot describing density changes against proximity to the colony edge with standard error marked.

non-breeding birds within the main breeding colony (Fig. 5). At both sites, an estimated breeding area determined from satellite imagery was larger than the breeding area calculated from drone imagery (Fig. 4). Satellite-image derived estimates when compared with all other methods, resulted in overestimation. Satellite imagery orthorectified over the DEM overestimated the least. This difference equated to an overestimate of 1,791 pairs (12.8%) at SLF and 17,826 pairs (23.9%) at SP, despite missing small sub-colonies at both sites on the satellite imagery which were easily visible using drone imagery. Using untrained observers versus an observer with ground familiarity equated to a further overestimate of 1,310 (9.4%) breeding pairs at SLF and 9,485 breeding pairs (12.4%) at SP. Using the drone-derived DSM to orthorectify the imagery was much more accurate than the DEMA

DSM, especially at Salisbury (14.2%), where part of the colony lies on a slope.

When count layers from manual and DSM methods were overlaid on the ortho imagery and visually compared, manually adjusted DSM counts missed the fewest birds and had no duplicates, this method was therefore considered to be the reference count to which other methods were compared. At SAB and SP where this count did not exist quadrat-based density counts were used but are likely overestimates.

Discussion

King penguins are a sentinel species in the Southern Ocean, tied to a narrow band of sub-Antarctic latitudes, currently vulnerable to ongoing climate change. They are

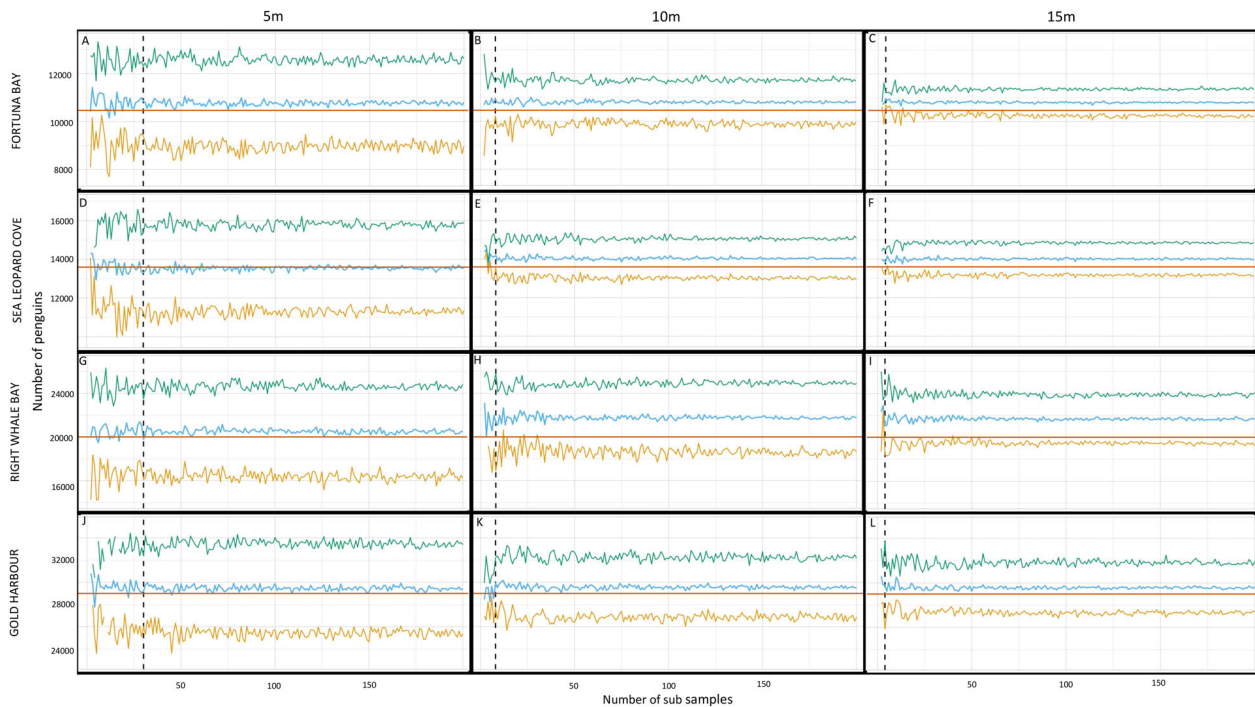


Figure 4. Number of king penguin breeding pairs estimated at Sea Leopard Fjord, Fortuna Bay, Right Whale Bay and Gold Harbour using multiple (between 1 and 200) 25, 100 and 225 m² quadrats. The mean population estimate (blue), upper (green) and lower (light orange) 95% confidence intervals are displayed. An actual number of breeding pairs (manually assisted DSM count) is represented by the solid horizontal line (dark orange). The black dashed line indicates the number of 5 × 5 (25 m²), 10 × 10 (100 m²) and 15 × 15 (225 m²) quadrats used (respectively 30, 8 and 4) for population estimate in Table 2 (closest value greater than 750 m²).

important predators in the Scotia Sea and integral to biogeochemical cycles within the region. This makes them a suitable candidate for long-term studies as ecological indicator species for monitoring broader ecosystem health. However, more efficient and accurate monitoring methods are first required.

Here, we report different approaches for estimating the number of breeding pairs of king penguins at six colonies in South Georgia. We tested a suite of established manual and novel post-processing methods for estimating colony size using both fixed-wing drones and satellite imagery. Our results are from the first use of fixed-wing drones in the sub-Antarctic and the first use of BVLOS flying at South Georgia.

Although field access is not necessary for satellite-based counts, drone-based methods provided the best combination of accuracy and efficacy, particularly with semi-automated DSM-based counts; these reliably estimated population size to within 1 percent of a manual count. As far as we know, this is the first use of the DSM-based approach for counting ground nesting birds, worldwide.

Full manual counts were the most time-consuming method, and although the clarity of the imagery gave

confidence in the count accuracy they underestimated breeding pairs when compared to the manually adjusted DSM count, observers suffered from counting fatigue and missed small numbers of birds. Some additional errors may be present at the colony edge due to the interpretation of breeding/non-breeding birds in this region. We estimated that a manual count of SAB would have taken over 350 hours. Manually adjusted DSM counts offered the most accurate count methodology. However, depending on the quality of the DSM, the supplementary counting of uncounted birds can be considerable. At SP, there were 11,000 additional birds compared to under 500 at FB, SLF and GH. At SLF, and GH, where the source imagery for the DSM was of high resolution, the automated DSM method counted 99% of penguin pairs. This method has considerable potential for future counting, not only of penguins but other taxa worldwide.

Corrected DSM-based counts were within 3% of the reference count, and closer than either satellite-image or quadrat-based density estimates. In our study, these counts took a similar level of effort as quadrat-based estimates. However, with greater image quality and DSM spatial resolution as with GH and SLF, the use of quadrats may not be necessary in the future. Using 225 m²

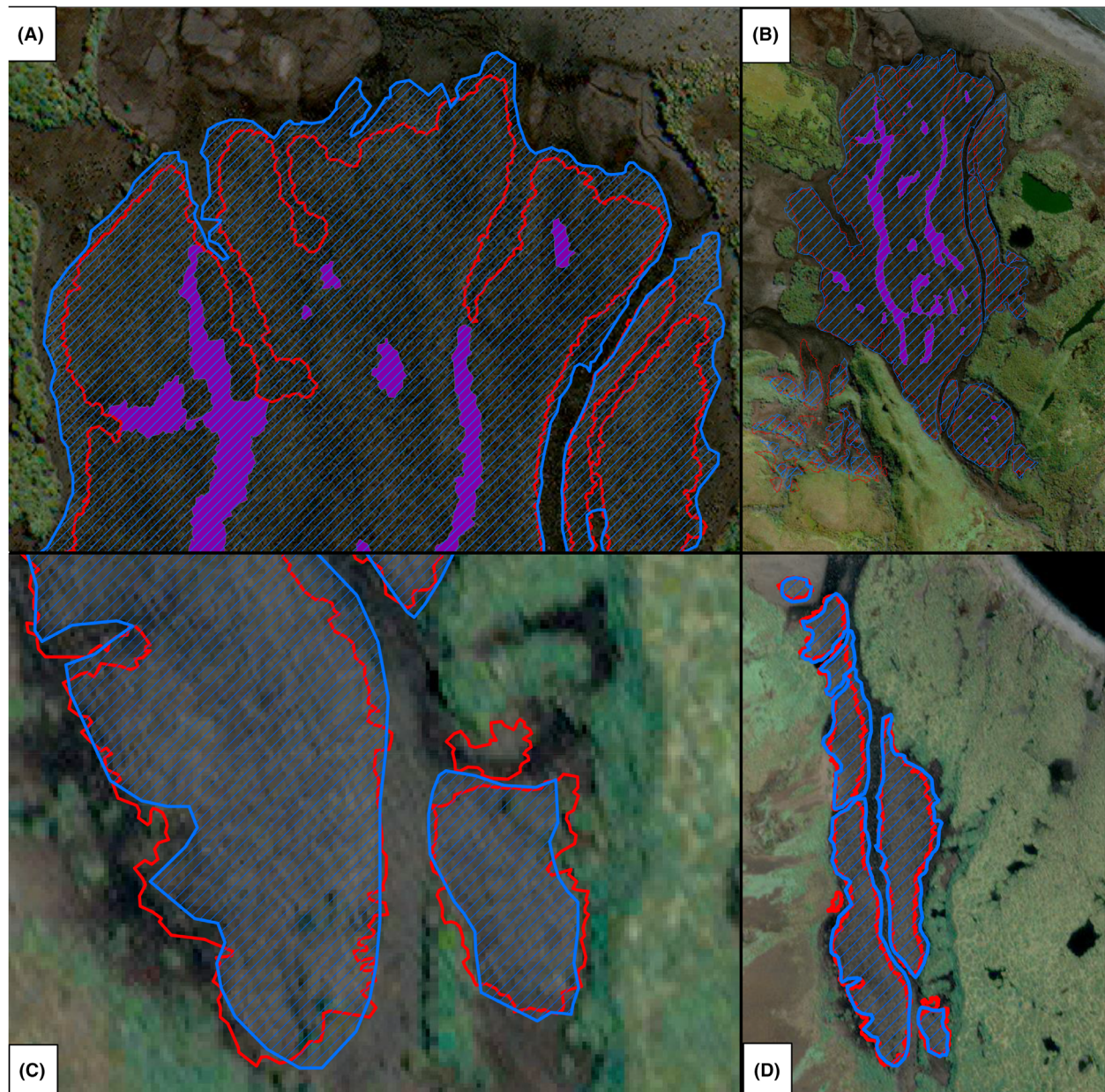


Figure 5. High-resolution satellite imagery (a, b) Salisbury Plain, and (c, d) Sea Leopard Fjord with drone-derived colony edge (red) and estimated edge from satellite imagery (blue) and colony gaps (purple). Maxar Products, WorldView-3 Image © 2022 Maxar Technologies.

quadrats to estimate density consistently overestimated colony size compared with DSM-based counts. Using 225 m^2 quadrats was also less accurate than automated counts and counts based on smaller sized quadrats. Fitting large uniform quadrats into irregular colonies is not always possible and often results in a low representation of the low-density, colony edge. Based on the random quadrat sampling simulations, 30, $5 \times 5 \text{ m}$ quadrats would sufficiently capture variation in density whilst producing accurate population estimates. The $5 \times 5 \text{ m}$

quadrats sub-sample a much smaller area than larger quadrats and are capable of capturing changes in nesting density variation efficiently. This was not affected by colony size and therefore 30 samples could be used at all sites. If effort is not a limiting factor, then sampling both buffers and cores separately will further increase the accuracy of counts.

Within this study, we made assumptions based on adjusting DSM counts to provide population estimates. The error observed within quadrats should be

representative of the entire colony. Future studies could investigate whether the correction factor can be calculated from smaller, 5×5 m quadrats (similar to the quadrat modelling sampling strategy). If successful, quadrat-based density estimates and DSM-adjusted estimates could be used in parallel to give two colony estimates from the same effort.

As discussed by Foley et al. (2020), when estimating population size using colony extent, knowing the density of breeding birds is necessary. All colony densities calculated within our study were below the 1.6 penguins per m^2 value observed by other studies (Foley et al., 2020; Gerum et al., 2018; Weimerskirch et al., 2018) and lay within the range (1.3–2.2) estimated by Williams (1995). Moreover, we show that density varies between and within sites, and emphasise that this should be accounted for with on-the-ground sampling otherwise overestimation is likely. For example, applying the density appropriate to SLF to SAB would have overestimated the population by 7,200 pairs (>5%). We note that average densities of 1.6 (Table S1), more appropriately equate to density in the colony core, which at SAB makes up less than 60% of the site. Thus, the best way to calculate density is with high-resolution aerial drone imagery. This variable density meant that parameter setting within Cloud Compare needed to be modified based on colony density; there are several other geomorphometric tools that should be investigated to develop this method.

Our data shows that density varies both between and within colonies (see also Gerum et al., 2018). Most significantly, there is a buffer zone at the colony edge (at least 3 m) where density is lower. Although core density will likely remain stable throughout the season, the buffer density will increase and decrease with the arrival of new breeders and breeding failure. The complexity of a breeding colony shape will impact this 'buffer effect' and lead to overestimates in colony size. These overestimates are proportional to the size of the buffer which can account for almost half of the colony area in some instances. To make density-based counts as accurate as possible this 'buffer zone edge effect' must be considered.

Many South Georgia king penguin colonies have increased from historical counts (Foley et al., 2018; Lewis Smith et al., 1979). One plausible explanation for the dramatic increase at SAB, which numbered fewer than 1000 pairs less than a hundred years ago (Lewis Smith et al., 1979), is an increase in available breeding space, following the rapid retreat of glaciers (Cook et al., 2010; Foley et al., 2018). Despite, these rapid increases, breeding density was lowest here, possibly due to large glacial deposits across the site. Our study also suggests that slope gradient impacts colony density, evidenced at RWB where lower breeding densities occurred where gradients

increased. However, further study is needed to substantiate this trend.

The three last colonies to be flown all had higher penguin densities, even though surveys were carried out within the window recommended by others (e.g. Bost et al., 2013; Foley et al., 2020). However, at SAB and SP large numbers of birds were still courting during our surveys, suggesting that flights at larger sites should be later in the season. A number of variables, including weather, colony size, and the breeding success of the previous year could impact the timing and number of breeding birds in a given year. We recognise that our counts are not reflective of the entire breeding population at these colonies. This also happens even when counting species with more regular annual breeding cycles. To understand full colony dynamics, those birds not present must be accounted for. King penguins have a complicated, multi-year breeding cycle which is impacted by many variables making monitoring difficult. Resulting models are associated with a wide range of errors and only long-term datasets will have statistical power to identify large population change (Foley et al., 2020). This emphasises the requirement for accurate methods with narrow confidence intervals, as reported here. The next step is annual replication to better inform demography models.

Satellite imagery does not require access to the colony; however, if long-term monitoring is to undertake counts at specific calendar dates each year (late January, early February in the case of this study) in remote sub-Antarctic locations where cloud cover will reduce image resolution (perhaps even preventing data acquisition), then a satellite-image-based approach may not be the best choice. Higher resolution imagery will be needed, especially for the colony edge, if the population is not to be overestimated (Foley et al., 2020). The overestimates in satellite-image-based counts came despite missing small sub-colonies at both sites which were clearly apparent from drone imagery. This error is due to the colony perimeter being occupied by non-breeding or courting birds (Stonehouse, 1960). At SP, an additional error (13%) came from not being able to see non-breeding birds within the main colony footprint as previously noted by Weimerskirch et al. (2018). These were present at all sites with the exception of SLF, highlighting that such errors are not consistent. If these non-breeding gaps exist to a similar extent between years, then site-based adjustments could be used for multiple years of satellite imagery. If the resolution of available satellite imagery increases in the future, some errors will be removed. However, errors associated with colony density may remain.

At both sites, using a high-resolution, drone-derived DSM significantly increased the accuracy of estimates

versus using the REMA DSM. This was especially true at SP; this greater difference is possibly a result of the west of the colony lying on a slope causing a difference between DSMs. DSMs from this project will be made available for future remote sensing work to reduce this effect.

Fixed-wing drones are powerful tools capable of efficiently mapping wildlife colonies, although caveats still exist. The downward-facing camera with no stabilisation meant that gusting winds could impact the pitch of the drone and lead to gaps in the imagery (and DSMs), as seen at SAB. To combat this, large overlaps were used between images (forward and side) which reduced the maximum area able to be surveyed within a single flight. Recently released sensors for the eBee X have gimbal stabilisation which will allow better image and DSM quality, and a reduction in the redundancy between images for even greater coverage.

BVLOS permits were necessary to overfly large colonies and allow remote locations for take-off and landing to minimise disturbance (Edney et al., 2023; Rümmler et al., 2016). Camera specification meant that the desired image resolution could be obtained from high altitudes, reducing flying times due to wider swath width. With hindsight, flying height should have been lower to allow for greater DSM resolution, particularly at SP and SAB, where conditions were poor.

To manually count breeding birds in large colonies is impractical, so other methods must be used. The most accurate of those we used were the semi-automated DSM counts and the 5×5 (25 m²) quadrat density estimates using both buffer and core subsamples. The next most accurate option, which also involved less effort was the thirty $\times 5 \times 5$ m sub-samples across the entire colony. Placement should be random but must include buffer areas. If using satellite imagery this should be done by observers with prior knowledge of the site and ideally in parallel with on-the-ground density estimates. If fully remote methodologies are to be used then a value less than 1.6 penguins per m² should be used which better represents actual density across the colony, whilst topography, buffer, and gradient should also be taken into account. Moreover, as colony boundaries are known to change across time (Trathan, unpublished), and are not easy to determine from satellite images (Fig. 4), fully remote methodologies still have important limitations.

Given recent observed and predicted colony declines north of the APF (Cristofari et al., 2018; Weimerskirch et al., 2018) understanding king penguin population trends in South Georgia remains important for understanding ecological change. Population counts of five of the six colonies listed here are significantly higher than those presented in previous studies, in line with recent

trends (Foley et al., 2018). However, caution is needed when interpreting isolated counts of king penguins due to their unique breeding chronologies (Foley et al., 2020). To better assess and inform king penguin conservation and allow ecological drivers of change to be identified, we encourage regular, long-term monitoring using methods we have tested in this study. The development of demographic models would also be informative (Foley et al., 2020).

Here we have demonstrated that DSMs can be used to successfully monitor wildlife populations. King penguins are large subjects that appear obvious on DSMs within this study, and this suggests that other species may also be targeted so long as they are larger than the resolution of the DSM. Looking at other seabird species, any bird that is colonial nesting may be considered a prospect for using DSMs for population monitoring. Northern gannets (*Morus bassanus*) are highly colonial nesting seabirds that have been previously surveyed by drone (Tyndall et al., 2024), often nesting on difficult-to-access offshore islands which this method would be suitable for. Furthermore, many seabirds are colonial nesters and this method could be easily applied as many are larger than a standard DSM resolution and have previously been surveyed with drone technology including cormorants (Polensky et al., 2022), gulls (Blight et al., 2019), and terns (Chabot et al., 2015). Beyond seabirds, this method could perceptibly be applied to any species that is larger than the surrounding environment, remains sedentary for any given period and has been surveyed from UAVs previously. Notably, this could be extended to include a variety of mammal species including seals (Mustafa et al., 2019), ungulates (Zabel et al., 2023) or even more solitary animals such as predators (Bushaw et al., 2019). However, as a study species reduces in size, differentiating them from the substrate becomes more difficult and it will be necessary to increase the resolution of the DSM, especially in more complex substrates. This could be done by flying the drone lower and by creating a higher resolution point cloud; however, this would need to ensure that disturbance to study animals is kept to a minimum. To distinguish the limits of this method, more investigation is needed with alternative species across multiple terrains but the authors believe it will be replicable with much smaller ground-nesting species.

Computer vision-based approaches for counting animals in drone imagery have a substantial amount of existing research but have not been compared in this study. Whilst general deep learning models for the detection of birds in imagery now exist (Weinstein et al., 2022), and computer vision models in general have proven to be accurate when compared to other count methods (e.g. Hayes et al., 2021; Torney et al., 2019) there are

limitations to their use. Whilst these approaches are undoubtedly cost-effective and quick once working, the development and training of models is a time-intensive process (Edney & Wood, 2021) that requires specialised skillsets. The aim of this project was to produce counts of king penguins for which we originally planned to use a combination of manual and density-based counts. The DSM approach was developed during the routine processing of imagery, and we, therefore, completed the density-based and manual counts where possible for the purpose of comparison. A clear future direction for the DSM method is a comparison with a computer vision-based approach using the same imagery.

This study identifies various limitations and advantages, in terms of effort and accuracy, of different counting approaches (see Figs S1 and S3). DSM-based counting, used in this study for the first time as a post-processing methodology is at least as accurate as traditional density-based and manual count methods whilst taking less time. This method will undoubtedly be applicable to other ground-nesting species worldwide. When used in conjunction with fixed-wing drones operated by BVLOS, these have the potential to revolutionise field-based counting of large ground-nesting colonial species such as penguins and make necessary long-term monitoring a reality.

Acknowledgements

We thank colleagues from the Government of South Georgia & the South Sandwich Islands, MV Pharos SG, and National Geographic Explorer for support and logistical help during fieldwork. Thanks also to colleagues from King Edward Point for support and assistance in the field and with maintaining equipment. We also thank the anonymous reviewers who greatly improved the manuscript.

Funding Information

Funding for this work came from the Darwin Plus scheme (DPLUS109).

Conflict of Interest

None of the authors has any conflicts of interest, financial or otherwise.

Ethics Statement

Ethical approval for this work was granted by the British Antarctic Survey Animal Welfare and Ethical Review Board (AWERB, #1071).

Data Availability Statement

All count data are contained within this manuscript. All raw imagery, orthorectified imagery and DSM files discussed in this paper (alongside metadata) are contained within the UK Polar Data Centre in the following DOIs: <https://doi.org/10.5285/dca60fc9-106a-4592-91e9-7a905056a679>; <https://doi.org/10.5285/e5a198a3-9d13-4f69-bc77-c00f0d732212>; <https://doi.org/10.5285/e4200c70-fce7-4cfb-9689-0ba079e0b884>; <https://doi.org/10.5285/bd6a8de8-fcf2-42fa-b0a6-1c940cd08b7f>; <https://doi.org/10.5285/7215b345-a75d-468f-a721-0c9d128e86dd>; <https://doi.org/10.5285/629882a1-7c29-46d0-bf2c-debbfdfeea22>; <https://doi.org/10.5285/3a09305c-6624-4322-8e99-dcb824fe26bc>

References

- Atkinson, A., Whitehouse, M.J., Priddle, J., Cripps, G.C., Ward, P. & Brandon, M.A. (2001) South Georgia, Antarctica: a productive, cold water, pelagic ecosystem. *Marine Ecology Progress Series*, **216**, 279–308. Available from: <https://doi.org/10.3354/meps216279>
- Barbraud, C., Delord, K., Bost, C.A., Chaigne, A., Marteau, C. & Weimerskirch, H. (2020) Population trends of penguins in The French Southern Territories. *Polar Biology*, **43**(7), 835–850. Available from: <https://doi.org/10.1007/s00300-020-02691-6>
- Belchier, M., Collins, M.A., Gregory, S., Hollyman, P. & Soeffker, M. (2022) From sealing to the MPA – a history of exploitation, conservation and management of marine living resources at the South Sandwich Islands. *Deep Sea Research Part II: Topical Studies in Oceanography*, **198**, 105056. Available from: <https://doi.org/10.1016/j.dsr2.2022.105056>
- Belyaev, O., Sparaventi, E., Navarro, G., Rodríguez-Romero, A. & Tovar-Sanchez, A. (2023) The contribution of penguin guano to the Southern Ocean iron pool. *Nature Communications*, **14**(1781), 1–9. Available from: <https://doi.org/10.1038/s41467-023-37132-5>
- Bestley, S., Ropert-Coudert, Y., Bengtson Nash, S., Brooks, C.M., Cotté, C., Dewar, M. et al. (2020) Marine ecosystem assessment for the Southern Ocean: birds and marine mammals in a changing climate. *Frontiers in Ecology and Evolution*, **8**, 338. Available from: <https://doi.org/10.3389/fevo.2020.566936>
- Blight, L.K., Bertram, D.F. & Kroc, E. (2019) Evaluating UAV-based techniques to census an urban-nesting gull population on Canada's Pacific coast. *Journal of Unmanned Vehicle Systems*, **7**(4), 312–324.
- Bost, C.-A.A., Delord, K., Barbraud, C., Cherel, Y., Pütz, K., Cotté, C. et al. (2013) King Penguin. In: Borborglu, P. (Ed.) *Penguins: natural history and conservation*. Seattle, WA: University of Washington Press, pp. 7–21.
- Brisson-Curadeau, É., Elliott, K. & Bost, C.A. (2023) Contrasting bottom-up effects of warming ocean on two

- king penguin populations. *Global Change Biology*, **29**(4), 998–1008. Available from: <https://doi.org/10.1111/gcb.16519>
- Budiharto, W., Chowanda, A., Gunawan, A.A.S., Irwansyah, E. & Suroso, J.S. (2019) A review and progress of research on autonomous drone in agriculture, delivering items and Geographical Information Systems (GIS). *Proceedings of 2019 2nd World Symposium on Communication Engineering, WSCE 2019*, 205–209. Available from: <https://doi.org/10.1109/WSCE49000.2019.9041004>
- Burger, A.E., Lindeboom, H.J. & Williams, A.J. (1978) The mineral and energy contributions of guano of selected species of birds to the Marion Island terrestrial ecosystem. *South African Journal of Antarctic Research*, **8**, 59–70.
- Bushaw, J.D., Ringelman, K.M. & Rohwer, F.C. (2019) Applications of unmanned aerial vehicles to survey mesocarnivores. *Drones*, **3**(1), 28.
- Chabot, D., Craik, S.R. & Bird, D.M. (2015) Population census of a large common tern Colony with a small unmanned aircraft. *PLoS One*, **10**, e0122588. Available from: <https://doi.org/10.1371/journal.pone.0122588>
- Chown, S.L. & Brooks, C.M. (2019) The state and future of Antarctic environments in a global context. *Annual Review of Environment and Resources*, **44**, 1–30. Available from: <https://doi.org/10.1146/annurev-environ-101718-033236>
- Cook, A.J., Poncet, S., Cooper, A.P.R., Herbert, D.J. & Christie, D. (2010) Glacier retreat on South Georgia and implications for the spread of rats. *Antarctic Science*, **22**(3), 255–263. Available from: <https://doi.org/10.1017/S0954102010000064>
- Côté, S.D. (2000) Aggressiveness in king penguins in relation to reproductive status and territory location. *Animal Behaviour*, **59**(4), 813–821. Available from: <https://doi.org/10.1006/anbe.1999.1384>
- Cristofari, R., Liu, X., Bonadonna, F., Cherel, Y., Pistorius, P., Le Maho, Y. et al. (2018) Climate-driven range shifts of the king penguin in a fragmented ecosystem. *Nature Climate Change*, **8**(3), 245–251. Available from: <https://doi.org/10.1038/s41558-018-0084-2>
- Boersma, P.D. (2008) Penguins as marine sentinels. *Bioscience*, **58**(7), 597–607. Available from: <https://doi.org/10.1641/B580707>
- Edney, A.J., Hart, T., Jessopp, M.J., Banks, A., Clarke, L.E., Cugniere, L. et al. (2023) Best practice for using drones in seabird monitoring and research. *Marine Ornithology*, **51**(2), 265–280.
- Edney, A.J. & Wood, M.J. (2021) Applications of digital imaging and analysis in seabird monitoring and research. *Ibis*, **163**, 317–337. Available from: <https://doi.org/10.1111/ibi.12871>
- Fenney, N., Hollyman, P., Coleman, J., Fox, A., Trathan, P. & Collins, M. (2024) *Aerial survey of the Fortuna Bay, South Georgia, king penguin colony during the 2021/22 season, flight number DPLUS_109_26 (Version 1.0)* [Data set]. NERC EDS UK Polar Data Centre. Available from: <https://doi.org/10.5285/dca60fc9-106a-4592-91e9-7a905056a679>
- Fenney, N., Hollyman, P., Coleman, J., Fox, A., Trathan, P. & Collins, M. (2024) *Aerial survey of the St Andrews Bay, South Georgia, king penguin colony during the 2021/22 season, flight number DPLUS_109_27 (Version 1.0)* [Data set]. NERC EDS UK Polar Data Centre. Available from: <https://doi.org/10.5285/e5a198a3-9d13-4f69-bc77-c00f0d732212>
- Fenney, N., Hollyman, P., Coleman, J., Fox, A., Trathan, P. & Collins, M. (2024) *Aerial survey of the Gold Harbour, South Georgia, king penguin colony during the 2021/22 season, flight number DPLUS_109_28 (Version 1.0)* [Data set]. NERC EDS UK Polar Data Centre. Available from: <https://doi.org/10.5285/e4200c70-fce7-4cfb-9689-0ba079e0b884>
- Fenney, N., Hollyman, P., Coleman, J., Fox, A., Trathan, P. & Collins, M. (2024) *Aerial survey of the Sea Leopard Fjord, South Georgia, king penguin colony during the 2021/22 season, flight number DPLUS_109_29 (Version 1.0)* [Data set]. NERC EDS UK Polar Data Centre. Available from: <https://doi.org/10.5285/bd6a8de8-fcf2-42fa-b0a6-1c940cd08b7f>
- Fenney, N., Hollyman, P., Coleman, J., Fox, A., Trathan, P. & Collins, M. (2024) *Aerial survey of the Right Whale Bay, South Georgia, king penguin colony during the 2021/22 season, flight number DPLUS_109_30 (Version 1.0)* [Data set]. NERC EDS UK Polar Data Centre. Available from: <https://doi.org/10.5285/7215b345-a75d-468f-a721-0c9d128e86dd>
- Fenney, N., Hollyman, P., Coleman, J., Fox, A., Trathan, P. & Collins, M. (2024) *Aerial survey of the Salisbury Plain, South Georgia, king penguin colony during the 2021/22 season, flight number DPLUS_109_32 (Version 1.0)* [Data set]. NERC EDS UK Polar Data Centre. Available from: <https://doi.org/10.5285/629882a1-7c29-46d0-bf2c-debbdfdea22>
- Fenney, N., Hollyman, P., Coleman, J., Fox, A., Trathan, P. & Collins, M. (2024) *Aerial survey of the Salisbury Plain, South Georgia, king penguin colony during the 2021/22 season, flight number DPLUS_109_33 (Version 1.0)* [Data set]. NERC EDS UK Polar Data Centre. Available from: <https://doi.org/10.5285/3a09305c-6624-4322-8e99-dcb824fe26bc>
- Foley, C.M., Fagan, W.F. & Lynch, H.J. (2020) Correcting for within-season demographic turnover to estimate the Island-wide population of king penguins (*Aptenodytes patagonicus*) on South Georgia. *Polar Biology*, **43**(3), 251–262. Available from: <https://doi.org/10.1007/s00300-020-02627-0>
- Foley, C.M., Hart, T. & Lynch, H.J. (2018) King penguin populations increase on South Georgia but explanations remain elusive. *Polar Biology*, **41**(6), 1111–1122. Available from: <https://doi.org/10.1007/s00300-018-2271-z>
- Freer, J.J., Tarling, G.A., Collins, M.A., Partridge, J.C. & Genner, M.J. (2019) Predicting future distributions of lanternfish, a significant ecological resource within the Southern Ocean. *Diversity and Distributions*, **25**(8), 1259–1272. Available from: <https://doi.org/10.1111/ddi.12934>

- Gerum, R., Richter, S., Fabry, B., Le Bohec, C., Bonadonna, F., Nesterova, A. et al. (2018) Structural organisation and dynamics in king penguin colonies. *Journal of Physics D: Applied Physics*, **51**(16), 1–8. Available from: <https://doi.org/10.1088/1361-6463/aab46b>
- Hayes, M.C., Gray, P.C., Harris, G., Sedgwick, W.C., Crawford, V.D., Chazal, N. et al. (2021) Drones and deep learning produce accurate and efficient monitoring of large-scale seabird colonies. *Ornithological Applications*, **123**(3), duab022. Available from: <https://doi.org/10.1093/ornithapp/duab022>
- Howat, I., Porter, C., Porter, C., Smith, B.E., Noh, M.-J. & Morin, P.J. (2022) *The reference elevation model of Antarctica – mosaics, version 2*. Harvard Dataverse, [Date Accessed May 2024] Available from: <https://doi.org/10.7910/DVN/EBW8UC>
- Le Bohec, C., Durant, J.M., Gauthier-Clerc, M., Stenseth, N.C., Park, Y.H., Pradel, R. et al. (2008) Reply to Barbraud et al.: king penguin population threatened by Southern Ocean warming. *Proceedings of the National Academy of Sciences of the United States of America*, **105**(26), E9. Available from: <https://doi.org/10.1073/pnas.0803656105>
- Lewis Smith, R.I., Tallowin, J.R.B., Lewis-Smith, R.I. & Tallowin, J.R.B. (1979) The distribution and size of king penguin rookeries on South Georgia. *British Antarctic Survey*, **49**, 259–276.
- Mattern, T., Rexer-Huber, K., Parker, G., Amey, J., Green, C.-P., Tennyson, A. et al. (2021) Erect-crested penguins on the Bounty Islands: population size and trends determined from ground counts and drone surveys. *Notornis*, **68**, 37–50. Available from: <https://doi.org/10.6084/m9.figshare.19709476>
- Matthews, L. (1929) The birds of South Georgia. *Discovery Reports*, **1**, 561–592.
- Meredith, M., Sommerkorn, M., Cassotta, S., Derksen, C., Ekaykin, A., Hollowed, A. et al. (2019) Polar regions. In: Pörtner, H.-O., Roberts, D.C., Masson-Delmotte, V., Zhai, P., Tignor, M., Poloczanska, E. et al. (Eds.) *IPCC special report on the ocean and cryosphere in a changing climate*. Cambridge: Cambridge University Press, pp. 203–320
- Millner, N., Cunliffe, A.M., Mulero-Pázmány, M., Newport, B., Sandbrook, C. & Wich, S. (2023) Exploring the opportunities and risks of aerial monitoring for biodiversity conservation. *Global Social Challenges Journal*, **2**, 2–23. Available from: <https://doi.org/10.1332/TIOK6806>
- Murphy, E., Watkins, J.L., Trathan, P.N., Reid, K., Meredith, M.P., Thorpe, S.E. et al. (2007) Spatial and temporal operation of the Scotia Sea ecosystem: a review of large-scale links in a krill centred food web. *Philosophical Transactions of the Royal Society, B: Biological Sciences*, **362** (1477), 113–148. Available from: <https://doi.org/10.1098/rstb.2006.1957>
- Mustafa, O., Braun, C., Esefeld, J., Knetsch, S., Maercker, J., Pfeifer, C. et al. (2019) Detecting Antarctic seals and flying seabirds by UAV. *ISPRS Annals of the Photogrammetry, Remote Sensing and Spatial Information Sciences*, **4**, 141–148.
- Olsson, O. & Brodin, A. (1997) Changes in king penguin breeding cycle in response to food availability. *Condor*, **99** (4), 994–997. Available from: <https://doi.org/10.2307/1370154>
- Olsson, O. & North, A.W. (1997) Diet of the king penguin *Aptenodytes patagonicus* during three summers at South Georgia. *Ibis*, **139**(3), 504–512. Available from: <https://doi.org/10.1111/j.1474-919X.1997.tb04666.x>
- Pascoe, P., Raymond, B., Carmichael, N. & McInnes, J. (2022) The current trajectory of king penguin (*Aptenodytes patagonicus*) chick numbers on Macquarie Island in relation to environmental conditions. *ICES Journal of Marine Science*, **79**(7), 2084–2092. Available from: <https://doi.org/10.1093/icesjms/fsac139>
- Petry, M.V., Basler, A.B., Valls, F.C.L. & Krüger, L. (2013) New southerly breeding location of king penguins (*Aptenodytes patagonicus*) on Elephant Island (maritime Antarctic). *Polar Biology*, **36**(4), 603–606. Available from: <https://doi.org/10.1007/s00300-012-1277-1>
- Pfeifer, C., Barbosa, A., Mustafa, O., Peter, H.U., Rümmler, M.C. & Brenning, A. (2019) Using fixed-wing UAV for detecting and mapping the distribution and abundance of penguins on the south Shetlands Islands, Antarctica. *Drones*, **3**(2), 1–22. Available from: <https://doi.org/10.3390/drones3020039>
- Polensky, J., Regenda, J., Adamek, Z. & Cisar, P. (2022) Prospects for the monitoring of the great cormorant (*Phalacrocorax carbo sinensis*) using a drone and stationary cameras. *Ecological Informatics*, **70**, 101726.
- Qian, Y., Humphries, G.R.W., Trathan, P.N., Lowther, A. & Donovan, C.R. (2023) Counting animals in aerial images with a density map estimation model. *Ecology and Evolution*, **13**, e9903. Available from: <https://doi.org/10.1002/ece3.9903>
- Rümmler, M.C., Mustafa, O., Maercker, J. et al. Measuring the influence of unmanned aerial vehicles on Adélie penguins. *Polar Biol* 39, 1329–1334 (2016). <https://doi.org/10.1007/s00300-015-1838-1>
- Scheffer, A., Bost, C. & Trathan, P. (2012) Frontal zones, temperature gradient and depth characterize the foraging habitat of king penguins at South Georgia. *Marine Ecology Progress Series*, **465**, 281–297. Available from: <https://doi.org/10.3354/meps09884>
- Scheffer, A., Trathan, P.N. & Collins, M. (2010) Foraging behaviour of king penguins (*Aptenodytes patagonicus*) in relation to predictable mesoscale oceanographic features in the polar front zone to the north of South Georgia. *Progress in Oceanography*, **86**(1–2), 232–245. Available from: <https://doi.org/10.1016/j.pocean.2010.04.008>
- Stonehouse, B. (1960) The King Penguin (*Aptenodytes patagonica*) of South Georgia. Breeding behaviour and development. *Falkland Islands Dependencies Survey Scientific Reports*, **23**, 1–81.

- Torney, C.J., Lloyd-Jones, D.J., Chevallier, M., Moyer, D.C., Maliti, H.T., Mwita, M. et al. (2019) A comparison of deep learning and citizen science techniques for counting wildlife in aerial survey images. *Methods in Ecology and Evolution*, **10**, 779–787. Available from: <https://doi.org/10.1111/2041-210X.13165>
- Trathan, P.N. (2008) Unpublished ground surveys of king penguin colonies on South Georgia.
- Trathan, P., Brandon, M. & Murphy, E. (1997) Characterisation of the Antarctic polar frontal zone to the north of South Georgia in summer. *Journal of Geophysical Research*, **102**(C5), 10483–10497.
- Trathan, P.N., Bishop, C., Maclean, G., Brown, P., Fleming, A. & Collins, M.A. (2008) Linear tracks and restricted temperature ranges characterise penguin foraging pathways. *Marine Ecology Progress Series*, **370**, 285–294. Available from: <https://doi.org/10.3354/meps07638>
- Trathan, P.N., Collins, M.A., Grant, S.M., Belchier, M., Barnes, D.K.A., Brown, J. et al. (2014) The South Georgia and the South Sandwich Islands MPA. In: Johnson, M.L. & Sandell, J. (Eds.) *Advances in marine biology*. Cambridge: Academic Press, pp. 15–78. Available from: <https://doi.org/10.1016/B978-0-12-800214-8.00002-5>
- Trathan, P.N., Daunt, F. & Murphy, E. (1996) *South Georgia: an ecological atlas*. Cambridge: British Antarctic Survey. [Accessed May 2024] Available from: http://www.antarctica.ac.uk/DYNAMOE/SG_GIS/SG_2_11
- Trathan, P.N. & Murphy, E.J. (2003) Sea surface temperature anomalies near South Georgia: relationships with the Pacific El Niño regions. *Journal of Geophysical Research: Oceans*, **108**(4), 1–10. Available from: <https://doi.org/10.1029/2000jc000299>
- Tyndall, A.A., Nichol, C., Wade, T., Pirrie, S., Harris, M.P. & Wanless, S. (2024) Quantifying the impact of avian influenza on the northern gannet colony of bass rock using ultra-high-resolution drone imagery and deep learning. *Drones*, **8**(2), 40.
- Watanabe, H., Shiomi, K., Sato, K., Takahashi, A., Handrich, Y. & Bost, C.-A. (2023) King penguins adjust their fine-scale travelling and foraging behaviours to spatial and diel changes in feeding opportunities. *Marine Biology*, **170**(3), 29. Available from: <https://doi.org/10.1007/s00227-022-04170-4>
- Weddell, J. (1825) *A voyage towards the south pole performed in the years 1822–1824*. London: Longman, Rees, Orme, Brown, and Green. Available from: <https://doi.org/10.5962/bhl.title.101503>
- Weimerskirch, H., Le Bouard, F., Ryan, P.G. & Bost, C.A. (2018) Massive decline of the world's largest king penguin colony at Ile aux Cochons, Crozet. *Antarctic Science*, **30**(4), 236–242. Available from: <https://doi.org/10.1017/S0954102018000226>
- Weimerskirch, H., Stahl, J.C. & Jouventin, P. (1992) The breeding biology and population dynamics of king penguins *Aptenodytes patagonica* on the Crozet Islands. *Ibis*, **134**(2), 107–117. Available from: <https://doi.org/10.1111/j.1474-919X.1992.tb08387.x>
- Weinstein, B.G., Garner, L., Saccomanno, V.R., Steinkraus, A., Ortega, A., Brush, K. et al. (2022) A general deep learning model for bird detection in high-resolution airborne imagery. *Ecological Applications*, **32**, e2694. Available from: <https://doi.org/10.1002/eap.2694>
- Williams, T.D. (1995) *The penguins*. Oxford University Press.
- Zabel, F., Findlay, M.A. & White, P.J. (2023) Assessment of the accuracy of counting large ungulate species (red deer *Cervus elaphus*) with UAV-mounted thermal infrared cameras during night flights. *Wildlife Biology*, **2023**(3), e01071.

Supporting Information

Additional supporting information may be found online in the Supporting Information section at the end of the article.

Figure S1. Decision-making workflow for selecting the most appropriate counting methodology.

Figure S2. Workflow for carrying out DSM-based automated count.

Figure S3. Number of king penguin breeding pairs estimated at Gold Harbour using multiple (between 1 and 200) 5×5 (25 m^2), 10×10 (100 m^2) and 15×15 (225 m^2) quadrats; colony (A-C), buffer (D-F), and core (G-I). The median population estimate (blue), upper (green) and lower (light orange) 95% confidence intervals are shown. Actual number of breeding pairs is represented by the solid horizontal line (dark orange). The black dashed line indicates the number (respectively 30, 8 and 4) used for population estimate in Table 2 (closest value greater than 750 m).

Table S1. King penguin breeding densities at colonies with DSM-assisted manual counts.